

## $(\alpha, n)$ reaction to high spin states in $^{14}\text{N}$ and $^{27}\text{Si}$

K. E. Luther, J. D. Brown, and R. T. Kouzes

*Joseph Henry Laboratories, Princeton University, Princeton, New Jersey 08544*

(Received 28 January 1988)

The  $0^\circ$  differential cross sections for the  $^{11}\text{B}(\alpha, n)^{14}\text{N}$ ,  $^{12}\text{C}(\alpha, n)^{15}\text{O}$ , and  $^{24}\text{Mg}(\alpha, n)^{27}\text{Si}$  reactions were measured at  $E_\alpha = 47.4$  MeV. Well-known states of high spin in  $^{15}\text{O}$  were used to determine the excitation energy of states in  $^{14}\text{N}$  and  $^{27}\text{Si}$ . Several states of high excitation energy in these nuclei are reported. The energies of these states are consistent with particle-hole weak coupling calculations for high spin states. Comparisons with previous experiments are made where possible.

The  $A(p, \pi^\pm)A+1$  reactions have received much attention in the past few years. A distinguishing feature of the  $(p, \pi)$  spectra on various nuclei is the selective population of a few states at high excitation energy.<sup>1</sup> The reaction is characterized by the high threshold energy and the unusually large amount of momentum transferred to the target nucleus.<sup>2</sup> The most widely accepted model of the near threshold  $(p, \pi)$  reaction mechanism is the two nucleon model (TNM), whereby the incident proton strikes a target nucleon, creating a pion. This model, therefore, predicts preferential excitation of states with high spin, especially those that have a two-particle-one-hole (2p-1h) configuration.

In studying the  $(\alpha, n)$  reaction, one may observe similar states as those populated by the  $(p, \pi)$  reaction and thereby elucidate the  $(p, \pi)$  reaction mechanism. The  $(\alpha, n)$  reaction at  $E_\alpha = 47.4$  MeV is expected to excite high spin states because, like the  $(p, \pi)$  reaction, it involves the transfer of a large amount of angular momentum, though not as large. Furthermore, because the  $(\alpha, n)$  reaction involves the transfer of three nucleons onto an  $A-2$  core, while  $(p, \pi)$  predominantly populates 2p-1h states on an  $A$  core, most of the configurations formed in  $(p, \pi)$  are accessible to  $(\alpha, n)$ . Some of these states have been studied successfully via the analog  $(\alpha, p)$  reaction,<sup>3</sup> yet a comparison between  $(p, \pi)$  and  $(\alpha, n)$  had not been investigated. The differential cross sections of the  $^{11}\text{B}(\alpha, n)^{14}\text{N}$  and  $^{24}\text{Mg}(\alpha, n)^{27}\text{Si}$  reactions were measured for comparison to the previously studied  $^{13}\text{C}(p, \pi^+)^{14}\text{C}$ ,  $^{13}\text{C}(p, \pi^-)^{14}\text{O}$ , and  $^{26}\text{Mg}(p, \pi^-)^{27}\text{Si}$  reactions.<sup>1,4</sup>

A 47.4 MeV  $^4\text{He}$  beam from the Princeton AVF ( $k=60$ ) cyclotron was focused on the target position inside the first dipole of the quadrupole-dipole-dipole-dipole magnetic spectrograph which was used to bend the beam away from the detector. The targets of enriched  $^{11}\text{B}$ ,  $^{24}\text{Mg}$ , and natural carbon were 0.49, 1.15, and 7.31 mg/cm<sup>2</sup> thick, respectively. The time-of-flight (TOF) of the neutrons was determined with an NE-213 liquid organic scintillator at zero degrees at 5.05 m from the target. Neutron-gamma identification was achieved by standard pulse shape analysis. A more complete description of the apparatus, electronics, and data acquisition system can be found in Ref. 5.

The resolution of the experiment was limited by the time spread of the cyclotron beam bursts which was about 2 ns as measured by the gamma peak in the TOF spectrum. This spread corresponds to an energy resolution which worsens with neutron energy from 350 keV

for 15 MeV neutrons to 1.5 MeV for 30 MeV neutrons. Due to the physical constraints on the flight path, the best resolution was obtained at zero degrees. Additionally, previous  $(\alpha, p)$  studies<sup>6</sup> on light nuclei have indicated that the differential cross section is largest at this angle for the higher spin states.

The absolute differential cross sections were computed with the detector efficiency as calculated by Anderson<sup>7</sup> using the Monte Carlo computer program described in Ref. 8. The estimated error in these calculations is less than one percent, however, it must be noted that the efficiency of the NE-213 detector is thought to vary considerably in the 20–40 MeV energy range.<sup>7</sup> Additionally, the error in peak fitting of the data to determine the yield was between 2% and 10%. The total error in the cross section is therefore estimated to be less than 15%.

The neutron TOF spectrum for the  $^{12}\text{C}(\alpha, n)^{15}\text{O}$  reaction is shown in Fig. 1. A comparison with previous studies<sup>9,10</sup> was used to determine the excitation energy of the most strongly populated states. This spectrum and the spectra from the  $(p, n)$  reaction to well-known states in  $^9\text{B}$ ,  $^{11}\text{C}$ , and  $^{12}\text{N}$  were used to determine the time per channel dispersion of the TOF spectra. The absolute TOF of each reaction was determined by the gamma peak in the spectrum.

Figure 2 shows the zero degree TOF spectrum for the  $^{11}\text{B}(\alpha, n)^{14}\text{N}$  reaction at  $E_\alpha = 47.4$  MeV. Table I lists the excitation energy of states of  $^{14}\text{N}$  as measured in this and

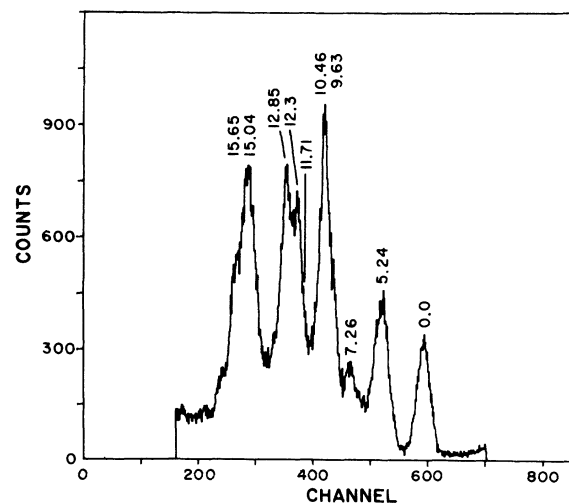


FIG. 1. Zero degree neutron time-of-flight spectrum for the  $^{12}\text{C}(\alpha, n)^{15}\text{O}$  reaction at  $E_\alpha = 47.4$  MeV.

previous experiments as well as the excitation energy of possible analog states in  $^{14}\text{C}$  and  $^{14}\text{O}$ . The measured cross section to discrete states and the spin, parity, and isospin assignments of those states are also listed there.

The ground state of the  $^{11}\text{B}$  nucleus has  $J^\pi = \frac{3}{2}^-$  and  $T = \frac{1}{2}$ . Therefore, both the  $T=0$  and  $T=1$  states of  $^{14}\text{N}$  can be reached by the  $(\alpha, n)$  reaction. The angular momentum mismatch of the  $(\alpha, n)$  reaction on  $^{11}\text{B}$  at 47.4 MeV is approximately  $2\hbar$  for the  $^{14}\text{N}$ ,  $J^\pi = 1^+$ , ground state which may explain the weak yield to that state. The momentum mismatch increases with the excitation energy of states in  $^{14}\text{N}$  and is about  $4\hbar$  for states at 24 MeV.

The two lowest energy peaks observed in the  $^{11}\text{B}(\alpha, n)^{14}\text{N}$  TOF spectrum are at approximately 5.2 and 8.6 MeV. Several states which could contribute to these peaks are not resolved due to the inherent time resolution of our system.

The first strong peak in the  $^{11}\text{B}(\alpha, n)^{14}\text{N}$  spectrum is at 14.71 MeV. Geesaman *et al.*<sup>11</sup> observed a state at 14.66(28) MeV in pion inelastic scattering and their shell model calculations predicted a  $J^\pi = 5^-$ ,  $T=0$  state at 14.89 MeV. Their assignment was made on the basis of the calculated cross section angular distribution which reproduced the magnitude and shape of the experimental

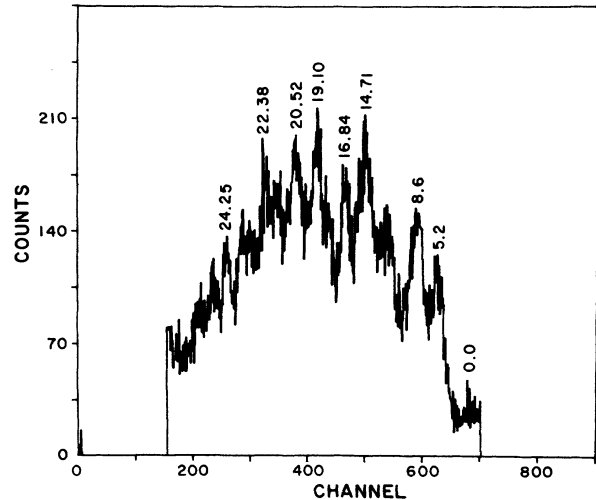


FIG. 2. Zero degree neutron time-of-flight spectrum for the  $^{11}\text{B}(\alpha, n)^{14}\text{N}$  reaction at  $E_\alpha = 47.4$  MeV.

distribution. The  $5^-$  state is thought to have a particle hole stretched configuration,  $[(d_{5/2})^1(p_{3/2})^{-1}]_{4^-}$ , coupled to the  $1^+$  ground state of  $^{14}\text{N}$ .

In a study of several transfer reactions to  $^{14}\text{N}$  and  $^{14}\text{C}$ ,

TABLE I. Energy levels of  $^{14}\text{N}$  and analog states in  $^{14}\text{C}$  and  $^{14}\text{O}$ . All energies are in MeV.

$^{14}\text{N}$		$^{14}\text{C}$			$^{14}\text{O}$	
$E_x$	This work $^{11}\text{B}(\alpha, n)^{14}\text{N}$ $d\sigma/d\Omega$ (mb/sr)	$E_x$	Others <sup>a</sup> $J^\pi; T$	Ref.	$^{13}\text{C}(p, \pi^+)^{14}\text{C}^k$ $E_x$ $J^\pi$	$^{13}\text{C}(p, \pi^-)^{14}\text{O}^k$ $E_x$ $J^\pi$
14.71	0.77	14.66	$5^-; 0$	b		
		14.73	$2^-$	c		
		14.81	$(2^-; 1)$	d		
		14.86		e		
		16.65	$4^+; 0+1$	f, g		
16.84	0.64	16.86	$5^-; 1$	h		
		16.91	$5^-; 1$	b	14.9	$5^-$
		16.91	$4^+; 0+1$	d		14.2
		16.92	$4^+; 0+1$	i, e, h		$5^-$
		16.92	$2^+; 0+1$	h		
		19.10	$3^-; 0+1$	h		
19.10	0.81	19.10	$3^-; 0+1$	h		
20.52	1.4	20.63	$4^+; 0+1$	h		
		20.65	$5^-; 0+1$	h		
21.72		21.53	$5^-; 0+1$	h		
		21.68	$4^+; 0+1$	h		
		21.8	$4^+; 0+1$	j		
		22.26	$4^+; 0+1$	h		
22.38		22.31	$5^-; 0+1$	h		
23.57		23.40	$5; 0+1$	h		
24.25	0.32				17.3	17.1
					$^{14}\text{C}(e, e')^{14}\text{C}^l$ $4^-$	
					22.1	22.0

<sup>a</sup>From Ref. 13 unless otherwise noted.

<sup>b</sup> $^{14}\text{N}(\pi, \pi')^{14}\text{N}$ , Ref. 11.

<sup>c</sup> $^{10}\text{B}(\alpha, \alpha)^{10}\text{B}$ .

<sup>d</sup> $^{14}\text{N}(e, e')^{14}\text{N}$ ,  $^{14}\text{N}(e, d)^{12}\text{C}$ .

<sup>e</sup> $^{11}\text{B}(^6\text{Li}, t)^{14}\text{N}$ , Ref. 12.

<sup>f</sup> $^{10}\text{B}(^6\text{Li}, d)^{14}\text{N}$ ,  $^{12}\text{C}(^6\text{Li}, \alpha)^{14}\text{N}$ .

<sup>g</sup> $^{12}\text{C}(^3\text{He}, p)^{14}\text{N}$ .

<sup>h</sup> $^{12}\text{C}(d, \alpha)^{10}\text{B}$ .

<sup>i</sup> $^{10}\text{B}(\alpha, p)^{13}\text{C}$ .

<sup>j</sup> $^{11}\text{B}(^3\text{He}, x)X$ .

<sup>k</sup>From Ref. 1.

<sup>l</sup>From Ref. 16.

Clark and Kemper<sup>12</sup> reported a  $T=0$  state at 14.850(30) MeV in  $^{14}\text{N}$  populated via the  $^{12}\text{C}(^6\text{Li},\alpha)^{14}\text{N}$  reaction. No analog state in  $^{14}\text{C}$  was found for the 14.85 MeV state of  $^{14}\text{N}$ , which is as expected. The most recent compilation<sup>13</sup> has reported a 14.66 MeV,  $J^\pi=2^-$  state [from  $^{10}\text{B}(\alpha,\alpha)^{10}\text{B}$ ,  $^{10}\text{B}(\alpha,n)^{13}\text{N}$ , and  $^{10}\text{B}(\alpha,p)^{13}\text{C}$  resonance studies], a 14.72 MeV, possibly  $(2^-;1)$  state (from electron inelastic scattering), and states at 14.86 and 14.92 MeV of unknown spin and parity. As the momentum mismatch for the  $(\alpha,n)$  reaction is large, it is construed that the main contribution to our observed peak at 14.71 MeV is from the  $(5^-;0)$  state at this energy.

The next prominent peak observed is at 16.84 MeV, in agreement with a state at 16.86 MeV strongly populated by pion inelastic scattering.<sup>11</sup> On the basis of shell model calculations, it was suggested that this is a  $(5^-;1)$  state. Those calculations also predict a  $(5^-;0)$  state at 18.0 MeV which is commensurate with a weak state observed via pion inelastic scattering at 17.46 MeV. In addition, electron inelastic scattering work<sup>14</sup> on  $^{14}\text{N}$  reports a  $J^\pi=5^-$ , probable  $T=1$  state at 16.910(20) MeV. Particle-hole coupling theory predictions<sup>15</sup> of the excitation energy of states with a  $(d_{5/2})^1(p_{3/2})^{-1}$  configuration indicate that the strongest  $J^\pi=5^-$ ,  $T=1$  state is at 16.91 MeV, which is in good agreement with the experimental value.

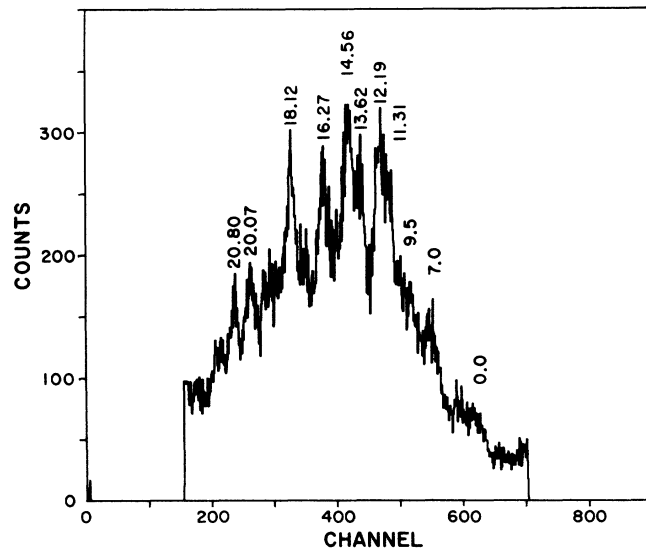


FIG. 3. Zero degree neutron time-of-flight spectrum for the  $^{24}\text{Mg}(\alpha,n)^{27}\text{Si}$  reaction at  $E_\alpha=47.4$  MeV.

Clark and Kemper<sup>12</sup> observed a state in  $^{14}\text{N}$  at 16.91 MeV and assigned it  $J^\pi=5^-$  following Geesaman *et al.*<sup>11</sup> States in  $^{14}\text{C}$  and  $^{14}\text{O}$  at 14.9 and 14.2 MeV, respectively, which are strongly populated by the  $^{13}\text{C}(p,\pi^+)^{14}\text{C}$  and

TABLE II. Energy levels of  $^{27}\text{Si}$  and  $^{27}\text{Al}$ . All energies in MeV; "w" indicates a weak state, "s" indicates a strong state.

$E_x$	This work $^{24}\text{Mg}(\alpha,n)^{27}\text{Si}$ $d\sigma/d\Omega$ (mb/sr)	$^{27}\text{Si}$			$^{27}\text{Al}$	
		$^{24}\text{Mg}(^6\text{Li},t)^a$ $E_x$	$^{26}\text{Mg}(p,\pi^-)^b$ $E_x$	$^{28}\text{Si}(p,d)^c$ $E_x$	$^{24}\text{Mg}(\alpha,p)^d$ $E_x$	$^{25}\text{Mg}(\alpha,d)^d$ $E_x$
11.31		11.23 <sup>s</sup>	11.2		11.52	11.28
		11.65 <sup>s</sup>		11.65 <sup>s</sup>	11.95	11.48
12.19	1.06		12		12.04	11.57
		12.25			12.54 <sup>s</sup>	12.02 <sup>s</sup>
		12.50			12.68	12.21 <sup>s</sup>
		12.75				12.51
		13.14				
13.62		13.40 <sup>w</sup>			13.53 <sup>w</sup>	
					13.65 <sup>w</sup>	13.64
		13.82			13.76 <sup>w</sup>	
14.56	1.15		14		14.12 <sup>s</sup>	14.06 <sup>s</sup>
		14.64 <sup>w</sup>				
				14.79		
		15.03		15.28		
		15.48		15.74		
16.27	0.50					16.88
					17.69	
18.12	0.35				19.61	
					19.79	
20.07	0.31					
20.80	0.27					
					21.2 <sup>w</sup>	

<sup>a</sup>Reference 18.

<sup>b</sup>Reference 4.

<sup>c</sup>Reference 19.

<sup>d</sup>Reference 20.

$^{13}\text{C}(p, \pi^-)^{14}\text{O}$  reactions, have been suggested<sup>1</sup> as probable analogs to the  $^{14}\text{N}$  state at 16.85 MeV. This suggests a  $J^\pi=5^-, T=1$  assignment to the triplet of analog states: 16.84 MeV in  $^{14}\text{N}$ , 14.9 MeV in  $^{14}\text{C}$ , and 14.2 MeV  $^{14}\text{O}$ . This is in agreement with weak coupling calculations for  $^{14}\text{C}$  and  $^{11}\text{B}(\alpha, p)^{14}\text{C}$  data.<sup>16</sup>

A strong state in  $^{14}\text{N}$  at 19.10 MeV was also observed. No state at this excitation is seen in the  $(\pi, \pi')$  spectrum. The tables<sup>13</sup> show a 19.10 MeV,  $J^\pi=3^-$  state with a width of approximately 900 keV, which is in agreement with the width of the peak we observe.

The next state was observed at 20.52 MeV. The compilation<sup>13</sup> lists two states which are found in the  $^{12}\text{C}(d, \alpha)^{10}\text{B}$  resonance work at this energy: a  $(4^+, 0+1)$  state at 20.63 MeV and a  $(5^-, 0+1)$  state at 20.65 MeV. The widths of the two states are 1100 keV and 610 keV, respectively, so that it is not possible on that basis to determine the spin and parity of the state observed at 20.52 MeV.

Between 22 and 24 MeV, several unresolved states are seen. However, it is possible that the small peak at 22.38 MeV could be the 22.31 MeV,  $J^\pi=5^-$  peak seen in the  $^{12}\text{C}(d, \alpha)^{10}\text{B}$  studies. The width given by the 22.31 MeV state is 600 keV, which is commensurate with our observations.

The state observed at 24.25 MeV has not been reported previously. It is expected to be a high-spin state with either a  $(d_{5/2})^3(p_{3/2})^{-1}$  or  $(d_{5/2})^2(p_{1/2})^1(p_{3/2})^{-1}$  configuration based on particle-hole weak coupling calculations.<sup>17</sup> There are possible analogs at 22.1 MeV in  $^{14}\text{C}$  seen via electron inelastic scattering,<sup>18</sup> and at 22.0 MeV in  $^{14}\text{O}$  seen in the  $^{13}\text{C}(p, \pi^-)^{14}\text{O}$  reaction.

The zero degree TOF spectrum for the  $^{24}\text{Mg}(\alpha, n)^{27}\text{Si}$  reaction at  $E_\alpha=47.4$  MeV is shown in Fig. 3. Table II reports the cross section to the discrete states of  $^{27}\text{Si}$  observed in this reaction. The table also displays the excitation energy of states of  $^{27}\text{Si}$  measured in previous studies and the energy levels of states in the isobaric analog nucleus,  $^{27}\text{Al}$ .

Strongly populated high spin states were seen at 7.0 and 9.5 MeV in  $^{27}\text{Si}$  via the  $^{26}\text{Mg}(p, \pi^-)^{27}\text{Si}$  reaction.<sup>4</sup> Though the resolution of the  $(\alpha, n)$  reaction studied is poor at these energies, evidence for states at these energies is apparent. The states are not nearly as strongly populated as they were by the  $(p, \pi^-)$  reaction, however,

they may be more prominent at angles where the momentum transfer is matched.

The 11.65 MeV state is thought to be a high spin state ( $J=\frac{9}{2}, \frac{11}{2}$ ) based on the cross section angular distribution.<sup>19</sup> States at higher excitation energies in  $^{27}\text{Si}$  up to 16 MeV have been observed previously.<sup>20,21</sup> In this experiment the excitation energies of several states between 11 and 21 MeV have been measured. The spins and parities of all of the  $^{27}\text{Si}$  states above 11 MeV have yet to be determined. Nonetheless, some general observations about the states observed in this experiment can be made. The only states that can be reached via the reaction studied are  $T=\frac{1}{2}$  states. The angular momentum mismatch in this region is  $5-7\hbar$ , so that the strongly excited states should have high spin, i.e.,  $\frac{9}{2}$  to  $\frac{15}{2}$ . It is expected that these states have an  $(f_{7/2})^3$  configuration. Particle-hole calculations<sup>17</sup> estimate the centroid of the  $(f_{7/2})^3$  states to be at approximately 14 MeV, so that this expectation is not unreasonable.

Above 10 MeV, the  $(p, \pi^-)$  spectrum shows only three weak peaks at approximately 11.2, 12, and 14 MeV. According to the TNM, states populated by the  $(p, \pi^-)$  reaction are high-spin, 2p-1h states. The highest spin states possible would have an  $(f_{7/2})^2(d_{5/2})^{-1}$  configuration, but  $(f_{7/2})^3$  states would not be populated unless the  $^{24}\text{Mg}$  ground state wave function is assumed to have an  $(f_{7/2})^2$  component.

In conclusion, it is observed that the  $^{12}\text{C}(\alpha, n)^{15}\text{O}$  reaction at zero degrees preferentially populated high spin states at high excitation. The  $^{11}\text{B}(\alpha, n)^{14}\text{N}$  reaction populates with comparable strength states that were seen in the  $(p, \pi^\pm)$  study of the  $^{14}\text{C}$  and  $^{14}\text{O}$  analogs.

The states preferentially populated by the  $^{26}\text{Mg}(p, \pi^-)^{27}\text{Si}$  reaction were not dominant in the  $^{24}\text{Mg}(\alpha, n)^{27}\text{Si}$  spectrum. The energies of several states of  $^{27}\text{Si}$  between 16 and 21 MeV are reported for the first time. The structures of these states have yet to be determined and warrant further investigation. However, the energies of these states are in agreement with the prediction for the location of states formed via the population of the  $(f_{7/2})$  level.

This work was supported in part by the National Science Foundation.

<sup>1</sup>T. G. Throwe, Ph.D. thesis, Indiana University Cyclotron Facility, 1984.

<sup>2</sup>S. E. Vigdor, Invited Talk at the International Symposium on Nuclear Spectroscopy and Nuclear Reactions, Osaka, Japan, 1984.

<sup>3</sup>Z.-J. Cao *et al.*, Phys. Rev. C **35**, 875 (1987).

<sup>4</sup>J. J. Kehayias *et al.*, Phys. Rev. C **33**, 1388 (1986).

<sup>5</sup>K. E. Luther, B. A. thesis, Princeton University, 1987.

<sup>6</sup>W. R. Falk *et al.*, Nucl. Phys. A**252**, 452 (1975); J. J. Hamill *et al.*, *ibid.* A**408**, 21 (1983).

<sup>7</sup>B. D. Anderson, private communication.

<sup>8</sup>R. A. Cecil, B. D. Anderson, and R. Madey, Nucl. Instrum. Methods **161**, 439 (1979).

<sup>9</sup>H. G. Bingham *et al.*, Phys. Rev. C **11**, 1913 (1975).

<sup>10</sup>D. J. Overway and W. C. Parkinson, Nucl. Phys. A**363**, 93 (1981).

<sup>11</sup>D. F. Geesaman *et al.*, Phys. Rev. C **27**, 1134 (1983).

<sup>12</sup>M. E. Clark and K. W. Kemper, Nucl. Phys. A**425**, 185 (1984).

<sup>13</sup>F. Ajzenberg-Selove, Nucl. Phys. A**449**, 1 (1986).

<sup>14</sup>J. C. Bergstrom *et al.*, Phys. Rev. C **29**, 1168 (1986).

<sup>15</sup>A. N. Golzov and N. G. Gonchaarova, Nucl. Phys. A**462**, 376 (1987).

<sup>16</sup>J. D. Brown *et al.* (unpublished).

<sup>17</sup>J. D. Brown and R. Sherr, private communication.

<sup>18</sup>M. A. Plum *et al.*, Phys. Rev. C **30**, 593 (1984).

<sup>19</sup>D. A. Miller, D. W. Devins, and J. P. Jones, Indiana University Cyclotron Facility Scientific and Technical Report, 1979, p. 92.

<sup>20</sup>Q. Li *et al.*, Indiana University Cyclotron Facility Scientific and Technical Report, 1982, p. 123.

<sup>21</sup>G. R. Smith *et al.*, Phys. Rev. C **30**, 593 (1984).